HHS Public Access

Author manuscript

Cell. Author manuscript; available in PMC 2017 June 02.

Published in final edited form as:

Cell. 2016 June 2; 165(6): 1361–1374. doi:10.1016/j.cell.2016.05.017.

Repression of the antioxidant NRF2 pathway in premature aging

Nard Kubben[1], **Weiqi Zhang**[2,3,#], **Lixia Wang**[2,4,7], **Ty C. Voss**[5], **Jiping Yang**[2,7], **Jing Qu**[4,7,#], **Guang-Hui Liu**[2,3,6,7,*], and **Tom Misteli**[1,*]

[1]National Cancer Institute, National Institutes of Health, Bethesda, MD 20892, USA

[2]National Laboratory of Biomacromolecules, Institute of Biophysics, Chinese Academy of Sciences, Beijing 100101, China

[3]FSU-CAS Innovation Institute, Foshan University, Foshan, Guangdong 528000, China

[4]State Key Laboratory of Stem Cell and Reproductive Biology, Institute of Zoology, Chinese Academy of Sciences, Beijing 100101, China

[5]High-Throughput Imaging Facility, National Cancer Institute, National Institutes of Health, Bethesda, MD 20892, USA

[6]Beijing Institute for Brain Disorders, Beijing 100069, China

[7]University of Chinese Academy of Sciences, Beijing, 100049, China

Abstract

Hutchinson-Gilford Progeria Syndrome (HGPS) is a rare, invariably fatal premature aging disorder. The disease is caused by constitutive production of progerin, a mutant form of the nuclear architectural protein lamin A, leading, through unknown mechanisms, to diverse morphological, epigenetic and genomic damage and to mesenchymal stem cell (MSC) attrition *in vivo*. Using a high-throughput siRNA screen we identify the NRF2 antioxidant pathway as a driver mechanism in HGPS. Progerin sequesters NRF2 and thereby causes its subnuclear mislocalization, resulting in impaired NRF2 transcriptional activity and consequently increased chronic oxidative stress. Suppressed NRF2 activity or increased oxidative stress are sufficient to recapitulate HGPS aging defects whereas re-activation of NRF2 activity in HGPS patient cells reverses progerin-associated nuclear aging defects and restores *in vivo* viability of MSCs in an animal model. These findings identify repression of the NRF2-mediated antioxidative response as a key contributor to the premature aging phenotype.

[*]Correspondence to: ; Email: mistelit@mail.nih.gov & ; Email: ghliu@ibp.ac.cn
[#]Co-Senior author

Author Contributions

NK and TM designed the study; GHL, WZ and JQ designed iPSC experiments; NK performed fibroblasts and HEK293FT-based experiments (Fig 1–5); WZ and JQ performed iPSC-based experiments (Fig 6); LW aided in iPSC culture and differentiation; JY constructed PLE4-caNRF2 and pLVTHM-shNRF2 vectors and aided in virus purification. TV aided in execution of the RNAi screen. NK, TM and GHL wrote the manuscript. All authors read and approved the manuscript.

Conflict of Interest

The authors declare no conflicts of interest.

Keywords

HGPS; Progerin; Aging; NRF2; Oxidative Stress

Introduction

Aging is a fundamental biological process linked to many common diseases, including cancer and cardiovascular disease. The naturally occurring human premature aging disorder HGPS is a powerful tool to study human aging (Gordon et al., 2014). In HGPS a de-novo mutation in the *LMNA* gene, encoding for the nuclear architectural proteins lamin A and C, activates an alternative RNA splice site, resulting in the expression of a lamin A mutant lacking 50aa, known as progerin, which undergoes incomplete posttranslational processing and consequently retains a farnesylated C-terminal CaaX motif (Gordon et al., 2014). Progerin is thought to also be relevant to the normal aging process, since sporadic usage of the same alternative splice site results in accumulation of progerin during physiological aging (Rodriguez et al., 2009; Scaffidi and Misteli, 2006). Progerin acts in a dominant fashion and causes a variety of cellular defects that compromise the integrity of nuclear architectural, heterochromatin maintenance, DNA repair and redox homeostasis, which has been ascribed to reduced levels of key proteins in these pathways (Mateos et al., 2013; Pegoraro et al., 2009; Scaffidi and Misteli, 2006; Viteri et al., 2010). At an organismal level *in vivo* attrition of MSCs, prone to the detrimental defects of progerin (Pacheco et al., 2014; Rosengardten et al., 2011; Scaffidi and Misteli, 2008), is thought to underlie HGPS tissue defects, in line with observations that HGPS induced pluripotent stem cells (iPSCs)-derived MSCs have reduced viability in hypoxic niches due to diminished capacity to respond to oxidative stress challenges (Liu et al., 2012; Liu et al., 2011a; Zhang et al., 2011).

Many of the cellular pathways affected in HGPS are highly interdependent, making it difficult to identify and distinguish cellular factors that are directly affected by progerin and drive HGPS etiology from those that are secondarily perturbed downstream of progerin and are secondary effects. For example, changes in lamin B1 levels observed in HGPS increase reactive oxygen species (ROS) (Malhas et al., 2009), which may compromise the nuclear envelope's integrity (Pekovic et al., 2011). At the same time, ROS may inflict DNA damage and decrease heterochromatin protein levels (Frost et al., 2014), which in turn may activate DNA damage signalling (Pegoraro et al., 2009). The complex interdependencies and the wide range of nuclear abnormalities observed in HGPS and in normal aging (Pegoraro et al., 2009; Zhang et al., 2015) points to the involvement of an upstream effector in the disease. A major goal in understanding HGPS and premature aging is the identification of primary driver mechanisms.

We have developed a cell-based high-throughput, high-content imaging siRNA screening assay to directly assess the involvement of individual factors in bringing about individual HGPS cellular phenotypes in mammalian cells. Using this system, we identify the antioxidant NRF2 pathway as a driver mechanism in HGPS.

Results

A targeted high-throughput RNAi screen to identify mediators of progerin-induced aging

We set out to identify human genes that drive the formation of progerin-induced aging defects. To this end, we generated human wild-type (WT) skin fibroblasts containing GFP-progerin under tight control of a doxycycline-inducible (Tet-on) promoter (See Experimental Procedures). GFP-progerin was nearly undetectable under normal growth conditions, but upon exposure to doxycycline was rapidly induced to levels comparable to endogenous lamin A (Fig S1A-B), resulting in the formation of nuclear defects typically observed in HGPS patient skin fibroblasts (Kubben et al., 2015; Musich and Zou, 2009; Scaffidi and Misteli, 2006), including nuclear shape distortions, decreased levels of the nuclear architectural proteins lamin B1 and LAP2, reduction of heterochromatin-associated HP1γ and tri-methylated lysine 27 on histone 3 (H3K27me3) (Fig S1A–C,F), and increased formation of DNA damage foci containing 53BP1 and serine-139 phosphorylated H2AX (γH2AX; Fig S1A,C,F).

Using this inducible model, we performed a high-throughput RNAi screen and searched for genes which prevent the occurrence of multiple HGPS phenotypes including loss of lamin B1, increase of γH2AX, as well as accumulation of GFP-progerin (Fig 1A). Given the widespread involvement of ubiquitin ligases in pathways affected in HGPS and aging (Low, 2011), as well as the observed selective degradation of a set of nuclear proteins in HGPS (Scaffidi and Misteli, 2006), we used a library containing 320 pools of 4 siRNAs targeting human ubiquitin E1, E2 and E3 ligases or their direct modulators (Table S3). The screen was conducted in quadruplicate in a 384-well format by reverse siRNA transfection of GFP-progerin fibroblasts while simultaneously inducing GFP-progerin expression for 96h (See Experimental Procedures; Fig 1A). Lamin B1, γH2AX and GFP-progerin levels were detected by immunofluorescence (IF) and automated high-throughput imaging of 500 – 2,000 cells per siRNA pool using custom-built image analysis algorithms (see Experimental Procedures). As a positive control, siRNA directed against GFP efficiently decreased induced GFP-progerin levels by 95% and prevented formation of lamin B1 and γH2AX defects, as opposed to a non-targeting siRNA that allowed for full development of the HGPS phenotype and served as negative control (Fig 1A, S1A,C). Z′-scores ranged from 0.15 to 0.74 depending on the cellular read-out (see Experimental Procedures). We identified 7 (2.2%) genes to affect multiple HGPS aging parameters (Fig 1B, S1J, Table S2–3). All candidates partially down-regulated progerin, 3 prevented formation of lamin B1 defects, and 4 prevented increased γH2AX foci formation. 4 of the 7 candidates (CAND1, WSB1, FBXO38 and FLJ25076) significantly down-regulated progerin and γH2AX protein levels, with a more moderate effect on lamin B1 defects (See Experimental Procedures; Table S2) and were further validated using siRNAs of a different targeting sequence and chemistry to exclude off-target effects. Amongst the validated targets, RNAi against CAND1 (cullin-associated NEDD8-dissociated protein 1) had the strongest effect and lowered progerin levels by 47%, prevented lamin B1 loss by 70% and γH2AX activation by 89% (all $p<0.05$; Table S2, S3, Fig 1C–D, S1F,I), making CAND1 a promising candidate for further investigation.

Loss of CAND1 function prevents and reverses HGPS aging defects

CAND1 is a member of several cullin-containing E3 ubiquitin ligase complexes. CAND1 does not possess ubiquitin ligase activity itself but functions to modulate the substrate specificity of the E3 ligase complexes (Chua et al., 2011). In addition to the screening phenotypes, CAND1 knockdown also prevented HGPS-associated reduction of LAP2, HP1γ, H3K27me3 and induction of 53BP1 foci (Fig 1D, S1G), while not affecting nuclear shape (Fig S1H). Importantly, this protective effect was not merely due to a reduction of progerin levels since lowering induction of progerin in shCTRL-treated cells to levels in shCAND1-treated cells, did not prevent the formation of most defects, except for a minor DNA damage protective effect (Fig S1K). CAND1 silencing (−94%; $p<0.05$; Fig S1D) was also sufficient to reverse already established aging defects in HGPS fibroblast, as it decreased endogenous progerin levels by 46%, restored lamin B1, HP1γ and LAP2 to WT levels, and partially rescued H3K27me3 defects (75%; all $p<0.05$; Fig 1E, S1G). γH2AX and 53BP1 levels remained unchanged (Fig 1E, S1G), in line with the reported resistance of DNA damage defects in HGPS cells to reversal (Liu et al., 2006). These data point to a role for CAND1 in a cellular pathway that is important in establishing and preventing a wide variety of aging defects triggered by progerin.

NRF2-ARE transcriptional activity is impaired in HGPS

A candidate pathway for the observed CAND1 effects was suggested by the RNAi screening results. Knockdown of the CAND1 interaction partner cullin 3 E3 ligase, but not of other CAND1 interacting cullin proteins tested in the screen, significantly prevented the γH2AX foci formation and moderately lowered GFP-progerin levels (−37%, Z=1.90; Table S3; Fig S1J. In addition, knockdown of RBX1, which interacts with various cullin proteins and is a member of the CAND1/cullin3 complex, prevented formation of lamin B1 defects (Table S3, Z= −2.14) but was slightly toxic. These results were of interest given that one of the major substrates of the CAND1/cullin3/RBX1 complex is the transcription factor NRF2 (Nuclear factor (erythroid-derived 2)-like 2), which has been implicated in organismal longevity and stress resistance by transcriptionally activating antioxidant genes upon binding to antioxidant responsive elements (ARE) motifs in their promoters (Lewis et al., 2010; Lo and Hannink, 2006; Ma, 2013). Indeed, CAND1 knockdown increased NRF2 protein levels (Fig S1E), in line with previous reports linking the cytoprotective effect of CAND1 knockdown to reduced CAND1/cullin3/ RBX1-mediated NRF2 protein degradation (Lo and Hannink, 2006).

Given that increased oxidative stress has been implicated in HGPS and normal aging (Viteri et al., 2010), we set out to determine the status of the NRF2-ARE axis in HGPS. Protein levels of NRF2 and KEAP1, which promotes NRF2 degradation via the CAND1/cullin3/ RBX1 pathway (Lewis et al., 2010), were unaffected by progerin in HGPS fibroblasts or upon induction of GFP-progerin in WT cells (Fig 2A–B, S2D). Small MAFs (musculoaponeurotic fibrosarcoma) proteins and CBP, two NRF2 transcriptional co-factors, were also unaffected (Fig 2A–B, S2D). Considering that the NRF2 pathway is also regulated at the level of nuclear import, we determined nuclear NRF2 protein levels, which were unchanged in HGPS cells in comparison to WT cells (Fig 2C–D), despite a 20% decrease in nuclear import promoting serine 40 phosphorylation (pSer40) of NRF2 (Bloom and Jaiswal,

2003), that could be corrected by progerin targeting shRNA (Fig S2C). Furthermore, the NRF2-activating compound sulforaphane increased nuclear NRF2 levels equally in the absence or presence of progerin (Fig S2A–B), indicating that NRF2 protein stability and nuclear-cytoplasmic shuttling is unaffected by progerin.

To fully assess the functional status of the NRF2-ARE pathway we measured its transcriptional activity using ARE-driven luciferase constructs (Wang et al., 2006). ARE-Luc activity was reduced by 51% in HGPS fibroblasts as a consequence of progerin since induction of GFP-progerin in WT cells resulted in a 77% inhibition of ARE-Luc activity ($p<0.05$; Fig 2E). Gene expression analysis demonstrated that abrogation of the NRF2-ARE axis was a global event since 213 out of 774 NRF2-ARE target genes were significantly repressed in HGPS versus WT cells (−0.31 Log2 fold change of average expression; $p<0.0001$; Fig 2F, S2F), while no global change was observed for non-NRF2 or HSF1-regulated control genes. Geneset enrichment analysis confirmed an enrichment of NRF2 target genes in WT versus HGPS cells (Table S4; Fig S2E). We conclude that progerin interferes with NRF2 function by impairing its transcriptional activity.

Progerin causes NRF2 mislocalization

To investigate potential mechanisms by which progerin interferes with the transcriptional function of NRF2, we probed its subnuclear distribution. Visualization of NRF2 protein, using a method established to visualize nuclear insoluble fractions (Voncken et al., 2005), revealed an increased accumulation of NRF2 at the nuclear periphery and intranuclear aggregates mirroring the distribution of progerin, both in progerin-inducible and HGPS cells, but not in uninduced and WT controls (Fig 3A–C, S3A–B). To test whether NRF2 mislocalization may be caused by a differential interaction of NRF2 with progerin compared to WT lamin A, we tested progerin-NRF2 interactions using an orthogonal One-STrEP (OST) pulldown assay in cellular extracts (Kubben et al., 2010). The interaction of nuclear OST-tagged NRF2 with progerin was strongly enhanced compared to WT lamin A (248%, $p<0.05$; Fig 3D). Conversely, OST-progerin pulled down significantly more NRF2 than OST-lamin A (142%; $p<0.05$; Fig 3E). For further validation we directly probed progerin-NRF2 interactions *in vitro* by testing the ability of recombinant NRF2 to bind to streptactin-purified, immobilized OST-lamin A and OST-progerin. In line with its co-localization and *in vivo* interaction, NRF2 preferentially bound to OST-progerin (275%; $p<0.05$; Fig 3F). These data suggest that progerin impairs the transcriptional activation of NRF2-ARE regulated antioxidants through sequestration of NRF2 away from its transcriptional targets.

NRF2 impairment causes oxidative stress and recapitulates the progeroid phenotype

To determine whether abrogation of NRF2 activity contributes to the progeroid phenotype, we investigated the effect of NRF2 knockdown in WT fibroblasts. NRF2 knockdown (−45%; Fig S4A–B) was sufficient to recapitulate all tested HGPS defects in WT cells. As expected, NRF2 RNAi increased progerin levels in WT inducible cells (Fig S4A), but further exacerbated nuclear defects in HGPS cells where NRF2 pathway activity is already suppressed without affecting progerin protein levels (Fig 4A–B, S4B–D), demonstrating that NRF2 affects the establishment of HGPS disease phenotypes by mechanisms other than modulating progerin levels.

In line with NRF2 impairment driving HGPS etiology, NRF2 knockdown in WT fibroblasts reduced expression of antioxidant genes, similarly to the effect of progerin (N=10, Fig S4E–F, S5E), thereby increasing ROS levels (+146%, $p<0.05$) comparably to HGPS cells (+79%; $p<0.05$; Fig 4C–D). Furthermore, elevated levels of oxidative stress itself, by H_2O_2 pro-oxidant treatment, was sufficient for WT fibroblasts to phenotypically mimic HGPS cells for all tested defects, with the anticipated exception of lamin B1 (Barascu et al., 2012) (Fig 4E, S4G,H,I). In line with the NRF2 RNAi experiments, H_2O_2 treatment of HGPS cells further worsened LAP2, HP1γ, H3K27me3, γH2AX and 53BP1 defects, as well as increased both lamin A (+55%) and progerin (+46%) levels, while not affecting lamin C levels (Fig 4E–F, S4G). Importantly, the observed increase in progerin levels did not account for lamin B1, LAP2, H3K27me3 and 53BP1 defects since individual cells expressing high levels of progerin had a nearly similar extent of HGPS-associated defects compared the total population of HGPS fibroblasts (Fig S4J). These results demonstrate that chronic oxidative stress due to impaired NRF2 activity, as found in HGPS cells, is sufficient to recapitulate cellular HGPS aging defects.

Re-activation of the NRF2 pathway reverses progerin-induced aging defects

To test whether NRF2 pathway re-activation ameliorates HGPS defects, we introduced constitutively activated NRF2 (caNRF2; See Extended Experimental Procedures) into WT and HGPS cells (Fig S5A). In line with CAND1 RNAi results, caNRF2 expression prevented the formation of all tested nuclear defects as well as lowered GFP-progerin levels (−60%, $p<0.05$; Fig S5B) in WT fibroblasts, and fully restored lamin B1, LAP2, HP1γ and H3K27me3 (Fig. 5A,C, S5F). NRF2 pathway re-activation in HGPS cells decreased progerin protein levels by 59% ($p<0.05$; Fig 5B), and reduced lamin A (−25%, $p<0.05$), without altering lamin C levels. In addition, we also tested the effect of four small molecule NRF2 activating agents on HGPS fibroblasts. Oltipraz (Magesh et al., 2012) ameliorated lamin B1 and HP1γ levels by 73% and 53% (100% = difference between WT and HGPS cells), respectively ($p<0.05$ Fig S5C), and showed some effect in reducing LAP2 and H3K27me3 defects (30–38%, $p>0.05$). CPDT restored lamin B1 levels and ameliorated HP1γ and H3K27me3 defects (52–79%, $p<0.05$), as did the compound AI-1 (Magesh et al., 2012). CPDT, however, increased γH2AX levels (+35% absolute change; $p<0.05$), which we did not observe for other tested compounds (Fig S5C). TAT-14, a cell-penetrating NRF2 stabilizing short peptide (Steel et al., 2012) restored HP1γ levels and ameliorated H3K27me3 defects (62%; $p<0.05$; Fig S5C). All beneficial effects of NRF2 activating compounds occurred without affecting progerin levels (Fig S5C).

caNRF2 expression also improved the expression of progerin-repressed NRF2-regulated antioxidant genes (N=10. Fig S5E), and lowered ROS levels in HGPS cells to only 39% of WT levels ($p<0.05$; Fig 5D). To test whether reducing oxidative stress itself is sufficient to reverse established HGPS aging defects, we treated HGPS patient cells with the broad-acting antioxidant N-acetyl cysteine (NAC). NAC treatment partially improved γH2AX (18% of WT/HGPS difference, $p<0.05$), restored LAP2 and HP1γ levels and ameliorated lamin B1 and H3K27me3 defects (38–54% of WT/HGPS difference; $p<0.05$; Fig 5E), without affecting endogenous progerin, lamin A or lamin C levels (FigS5D). The observation that increased NRF2 activity by caNRF2 expression or CAND1 knockdown in

WT cells does not alter lamin B1, LAP2, HP1 γ, H3K27me3, γH2AX and 53BP1 protein levels (Fig S5G–H), but as expected lowers ROS levels (Fig S5I), further indicates that NRF2 pathway re-activation specifically corrects HGPS patient cellular defects, while not affecting the physiological levels of key proteins in these pathways. Overall, these data demonstrate that restoration of the impaired NRF2 pathway in HGPS patient cells ameliorates aging defects *in vitro* by lowering oxidative stress.

NRF2 pathway activation restores in vivo viability of HGPS mesenchymal stem cells

A prominent *in vivo* defect in HGPS is the reduced ability of MSCs to respond to oxidative stress, limiting their viability *in vivo* (Zhang et al., 2011) and contributing to reduced stem cell pools in HGPS (Pacheco et al., 2014; Rosengardten et al., 2011). To test the effect of NRF2 pathway modulation on HGPS MSCs, we generated iPSCs from HGPS patient fibroblasts (henceforth HGPS-iPSCs; See Experimental Procedures), and their isogenic control in which the *LMNA* C1824T mutation had been genetically corrected (GC-iPSCs; Fig S6A)(Liu et al., 2011b). As expected, since *LMNA* is inactive in iPSCs (Constantinescu et al., 2006; Liu et al., 2011a; Liu et al., 2011b) (Fig S6A), expression of NRF2-regulated antioxidants was not downregulated in HGPS-iPSCs compared to GC-iPSCs (Fig 6A). However, in line with progerin impairment of NRF2 activity, re-activation of the *LMNA* gene upon differentiation of iPSCs into MSCs reduced NRF2-target gene expression in HGPS-iPSC-MSCs compared to GC-iPSC-MSCs (Fig 6A, S6B–C). This effect was a direct consequence of progerin expression since induced GFP-progerin expression in GC-iPSC-MSCs similarly reduced NRF2 target gene expression (Fig S6D–E). Reduced NRF2 activity was sufficient to mimic HGPS defects since NRF2 knockdown in GC-iPSC-MSCs decreased expression of NRF2 antioxidant genes (Fig 6B), increased oxidative stress (Fig 6C), reduced levels of lamin B1, LAP2, and HP1γ proteins ($p<0.05$; Fig 6D, S6G), increased frequencies of senescence associated β-galactosidase (SA β-gal) positive cells (Fig 6E) and ultimately reduced cell survival (Fig 6F) comparable to HGPS-iPSC-MSCs (Fig S6F–H). Conversely, expression of caNRF2 in GC-iPSC-MSCs increased, as expected, expression of NRF2 antioxidant genes and thereby lowered ROS levels (Fig 6H, S6I). To test the effect of the progerin-NRF2 pathway *in vivo*, we used an established animal model (Zhang et al., 2011) in which MSCs are implanted into the *tibialis anterior* muscle and engraftment and survival is measured (Pan et al., 2016; Zhang et al., 2015) (See Experimental Procedures). As expected by our *in vitro* observations, the presence of progerin in HGPS-iPSC-MSCs or knockdown of NRF2 in GC-iPSC-MSCs resulted in increased stem cell attrition in the *in vivo* niche ($p<0.05$; Fig 6L). We finally tested whether restoration of NRF2 pathway activity in HGPS-iPSC-MSCs rescued the observed HGPS defects. Overexpression of caNRF2 (E82G, See Experimental Procedures) or Oltipraz-mediated NRF2 activation in HGPS-iPSC-MSCs increased expression of NRF2-regulated antioxidants (Fig 6G), decreased ROS levels (Fig 6H), rescued HGPS nuclear defects (Fig 6I) and reduced the number of apoptotic (Fig 6J) and SA β-gal-positive cells (Fig 6K). Similarly, knockdown of CAND1 in HGPS-iPSC-MSCs reactivated all tested NRF2-target genes (Fig S6J–K). Importantly, NRF2 pathway re-activation by expression of caNRF2 restored the *in vivo* viability of HGPS-MSCs (Fig 6L). A similar effects was observed by pre-treatment of cells with the mild NRF2 inducer Oltipraz (Fig 6L) indicating that the NRF2-mediated rescue effect is not due

to massive hyperactivation of the pathway. These data from an HGPS-relevant animal model support an *in vivo* role of NRF2 as a driver in HGPS pathology.

Discussion

The lamin A mutant isoform progerin causes extensive architectural, epigenetic, redox and DNA damage defects in the premature aging syndrome HGPS (Gordon et al., 2014; Scaffidi and Misteli, 2006; Viteri et al., 2010). It is unclear how progerin triggers these defects and discovery of HGPS driver mechanisms is crucial to a molecular understanding and the identification of therapeutic targets of premature and normal aging. Using a high-throughput, high-content cell-based assay we identify impairment of the longevity-promoting transcription factor NRF2 by progerin as a driver mechanism in HGPS etiology.

NRF2 is a major stress responder that transcriptionally activates antioxidant and cytoprotective genes through binding to ARE motifs (Lewis et al., 2010). The sum of our results delineates a mechanism by which progerin sequesters NRF2, and in this way reduces its availability for transcriptional activation of antioxidant genes, resulting in elevated oxidative damage and consequentially an array of HGPS defects. Given that progerin is a highly expressed long-lived protein (Boisvert et al., 2012), whereas NRF2 is low in abundance and short-lived (McMahon et al., 2004), progerin/NRF2 sequestration is expected to drastically reduce the availability of NRF2 for the formation of functional transcription factor complexes at ARE motifs. In agreement, we find that experimental elevation of NRF2 levels in HGPS cells restored NRF2 pathway activity, further suggesting that the availability of NRF2, and not of other NRF2/ARE complex co-factors, is limited in HGPS.

A likely scenario, based on this study and others, for how increased ROS levels contribute to HGPS etiology suggests that aberrant NRF2/progerin interaction reduces expression of antioxidants, increases ROS levels, thereby causing loss of heterochromatin and increased levels of DNA damage (Frost et al., 2014; Pegoraro et al., 2012; Richards et al., 2011). We hypothesize that the elevated oxidative stress in HGPS cells is the result of increased ROS formation, due to defective mitochondrial oxidative phosphorylation (Rivera-Torres et al., 2013), a pathway whose integrity is maintained by the progerin-impaired NRF2 target NQO1 (Kwon et al., 2012), as well as a diminished ROS counteracting antioxidative capacity due to impaired NRF2 activity. Subsequently, increased ROS levels can cause a severe loss of heterochromatin (Frost et al., 2014), which precedes, and by itself is sufficient to activate, DNA damage signaling as observed in progerin inducible fibroblasts (Pegoraro et al., 2009). The fact that NRF2 activation fully prevents γH2AX and 53BP1 foci formation upon progerin induction in a WT background, but does not reduce these defects in HGPS cells, suggests that progerin renders DNA damage foci partially irreparable through NRF2 pathway independent mechanisms, in line with previously observed minimal effects in this regard for farnesyl-transferase inhibitors (Liu et al., 2006) and NAC (Richards et al., 2011). Similarly, nuclear shape alterations, whose formation was prevented by NRF2 activation in progerin inducible WT cells, but were not reversed once established in HGPS patient cells, may be due to insufficient reduction of progerin levels by caNRF2.

Several lines of evidence support the conclusion that the protective function of NRF2 in HGPS is largely independent of an effect on progerin levels. First, lowering ROS levels in HGPS fibroblasts by NAC antioxidant treatment ameliorates HGPS defects without lowering progerin levels. Second, further impairment of NRF2 activity in HGPS fibroblasts by NRF2 knockdown worsens all tested defects without altering progerin protein levels. Third, using single cell level analysis we observed that even a 50% above average increase in progerin levels in HGPS patient cells did not account for the increased defects observed upon H_2O_2 pro-oxidant treatment. Fourth, increased oxidative stress levels through NRF2 knockdown or H_2O_2 treatment in WT cells was sufficient to mimic HGPS defects in the absence of progerin. Fifth, when comparing two cell populations with similar progerin levels, but one with activated NRF2 signaling due to CAND1 knockdown, the reduction of progerin alone was insufficient to prevent the formation of other nuclear defects. A possible mechanism as to how NRF2 may decrease progerin comes from previous observations that the NRF2-ARE pathway also transcriptionally activates 20S proteasome subunits to aid in the clearance of ROS damaged proteins (Pickering et al., 2013). A plausible scenario is that re-activation of NRF2 activity in HGPS cells increases the capacity of the proteasome system, which is slightly attenuated in HGPS cells (Viteri et al., 2010), and thereby aids in clearing of ROS damaged proteins as well as progerin aggregates.

Our results are in line with observations at the organismal level, which have demonstrated a contribution of the NRF2 pathway to multiple aspects of premature aging. Genetic disruption of the *Nrf2* gene decreases the lifespan of female mice (Yoh et al., 2001), and hypomorphic mutants of SKN-1, the *C. elegans* NRF2 homologue, shorten *C. elegans* lifespan nearly two-fold (An and Blackwell, 2003). Furthermore, *Nrf2* knockout mice show decreased adipogenic differentiation and HDL levels (Tanaka et al., 2008), intriguingly similar to the global loss of adipose tissue and altered blood-lipid profiles in HGPS patients (Gordon et al., 2005), and in addition suffer from aging-associated skeletal muscle wasting, retinopathies and dermal photo-aging (Hirota et al., 2011; Miller et al., 2012; Zhao et al., 2011). As expected, reported phenotypes in NRF2 targeted mice are milder than in HGPS mice models (Chan et al., 1996), most likely due to redundancy and biological differences between complete genetic gene disruption versus a hypomorphic effect on NRF2 in HGPS.

Although our primary goal was to identify HGPS driver mechanisms, our observations suggest that restoration of NRF2 activity may offer a novel therapeutic strategy for HGPS. Clinical activation of NRF2 in HGPS patients may increase bone mineral density, which is reduced in HGPS patients (Rankin and Ellard, 2006) and has been observed in *Nrf2* knockout mice (Ibanez et al., 2014). NRF2 activation may also decrease the prevalence of atherosclerotic lesions and stroke (Li et al., 2009), the main causes of death in HGPS patients (Gordon et al., 2014). Cardiovascular protective effects may further occur due to NRF2 inhibiting NFkB inflammatory responses (Li et al., 2008), which are detrimental to HGPS (Osorio et al., 2012). Given that increased NRF2 activity restored *in vivo* HGPS-iPSC-MSC viability, we expect NRF2 activation to counteract the premature exhaustion of adult stem cell populations that occurs in HGPS patients (Halaschek-Wiener and Brooks-Wilson, 2007) due to their diminished capacity to respond to oxidative challenges in their hypoxic niches (Liu et al., 2012; Liu et al., 2011a; Zhang et al., 2011). Further beneficial effects may originate from the fact that adult stem cells are highly dependent on NRF2

activity to maintain self-renewal ability and lineage commitment (Murakami et al., 2014; Pan et al., 2016), and show altered differentiation upon reduction of NRF2-regulated MnSOD antioxidant (Michaeloudes et al., 2011) and elevated ROS levels (Mateos et al., 2013).

Due to these health-promoting effects of NRF2, identification of NRF2 activating small molecular compounds is a high-value target in drug discovery (Magesh et al., 2012). Our observation that the FDA-approved drug Oltipraz, used for treatment of liver fibrosis, as well as other experimental NRF2 activating compounds improved multiple aging defects in HGPS cells further indicates the potential of NRF2 activating drugs as a novel type of treatment in HGPS. In this light it is also noteworthy that both sulforaphane and resveratrol, which alleviate HGPS symptoms (Gabriel et al., 2015; Liu et al., 2012), are dependent on NRF2 for their general health promoting effects in non-HGPS animal models (Ungvari et al., 2010; Zakkar et al., 2009). Finally, and maybe most intriguingly, the recent finding that lamin A mutants that cause muscular dystrophy lead to cytoplasmic KEAP1 aggregation, increased NRF2 activity and reductive stress (Dialynas et al., 2015), raises the possibility that defective NRF2 pathway activity may not just be a driver of HGPS, but a common denominator amongst laminopathies.

Experimental Procedures

Cell lines and treatments

hTert immortalized doxycycline GFP-progerin inducible human skin fibroblasts (P1 cells) were generated and induced (96 hours) as described (Kubben et al., 2015). Human HGPS-iPSCs (C1824T *LMNA* mutation) and their gene-corrected isogenic counterparts (GC-iPSC; no *LMNA* mutation) were generated as described (Liu et al., 2011b). iPSC MSC differentiation was performed using established protocols (Duan et al., 2015; Zhang et al., 2015). Primary HGPS patient skin fibroblasts (Coriell Cell Repository (CCR), AG01972 and AG06297), and age-matched control cell lines (American Type Culture Collection, CRL-1474; CCR, GM00038) were used under conditions as previously described (Pegoraro et al., 2009). Cell treatments included AI-1 (125μM), CPDT (60μM), H_2O_2 (100, 125 and 250μM), NAC (10 mM), oltipraz (20, 100 μM), and sulforaphane (5μM), TAT-14 (100 μM). All compounds were purchased from Sigma, except TAT-14 (Millipore). H_2O_2, NAC and TAT-14 were dissolved in PBS, all others in DMSO. Media with compounds were replaced every 48 hours, except for H_2O_2 which was left unreplaced for 96 hours (Fig 4), or was replaced with vehicle containing medium after one hour of stimulation (Fig S4G).

siRNA transfection in 384-well format

Reverse siRNA transfections were carried out in quadruplicate in a 384-well format (Perkin Elmer Cell carrier plates) in presence of doxycycline (1μg/ml) as described (Pegoraro et al., 2009) with pooled siRNA oligos (50nM; 4 siRNAs/target) from the Dharmacon siGENOMESMARTpool siRNA Human Ubiquitin Conjugation subset 1 and 2 libraries. Positive and negative controls consisted of GFP-targeting and non-targeting siRNA (50nM; Ambion, #AM4626, #AM4611G), respectively. Transfected cells were incubated overnight,

after which 60μl of antibiotic and doxycycline (1 μg/ml) containing medium was added and cells were incubated for another 3 days (37°C, 5% CO_2).

High-throughput high-content imaging analysis

IF staining was performed (See Extended Experimental Procedures), after which cells were imaged in a single optimal focal plane (24 fields/ well, 20x water immersion objective) on an Opera high-throughput spinning-disk confocal microscopy system (Perkin Elmer), using sequential acquisitions with a 405/640, 488 and a 568 nm excitation laser. IF stainings were analyzed at the singular cell level with a customized algorithm (Kubben et al., 2015) using DAPI-based nuclear segmentation to quantify the total nuclear intensity for all indicated targets, and a contrast-based algorithm to detect 53BP1 foci numbers and total integrated intensity for γH2AX foci (Kubben et al., 2015). 500–2000 cells were analyzed per condition, and quantifitions were depicted as an average of the total cell population. iPSC IF experiments were captured with a Leica SP5 confocal microscope, and total nuclear intensity was quantified with ImageJ software. Normalized Z-score RNAi screen values were calculated using CellHTS2 (Pegoraro et al., 2012). Z′-scores for the assays' parameters were 0.15 (lamin B1), 0.38 (γH2AX) and 0.74 (progerin). siRNA pools with cell numbers above 50% of the negative control, and with a Z-score <−1.65 for lamin B1 or >1.65 for γH2AX, together with a Z-score >2.0 for progerin, were selected initial candidates, out of which the strongest candidates (Z-score <−2.0 for combined laminB1 and γH2AX effects, See Table S2) were pursued for secondary validation using On-Target Plus pooled siRNAs (Dharmacon, 4/target).

Statistical analysis

All RNAi screening follow-up experiments are depicted as averages of 3 biological replicates, each consisting of at least 3 technical replicates, unless stated otherwise, and analyzed by student's t-test in Graphpad Prism.

Supplementary Material

Refer to Web version on PubMed Central for supplementary material.

Acknowledgments

We thank Misteli lab members, P. Scaffidi, Y. Xiong and J.C. Izpisua Belmonte for sharing feedback, data and reagents. The Liu and Qu labs were supported by the National Basic Research Program of China (973 Program, 2015CB964800; 2014CB910503), the Strategic Priority Research Program of the Chinese Academy of Sciences (XDA01020312), the National High Technology Research and Development Program of China (2015AA020307), the National Natural Science Foundation of China (81330008; 31222039; 31201111; 81371342; 81300261; 81300677; 81271266; 81471414; 81422017; 81401159), the Program of Beijing Municipal Science and Technology Commission (Z151100003915072), the Beijing Natural Science Foundation (7141005; 5142016), the Key Research Program of the Chinese Academy of Sciences (KJZDEW-TZ-L05), and the Thousand Young Talents program of China. The Misteli lab was supported by the Intramural Research Program of the NIH/NCI/ CCR and a Progeria Research Foundation grant.

References

An JH, Blackwell TK. SKN-1 links C. elegans mesendodermal specification to a conserved oxidative stress response. Genes & development. 2003; 17:1882–1893. [PubMed: 12869585]

Andersen JS, Lyon CE, Fox AH, Leung AK, Lam YW, Steen H, Mann M, Lamond AI. Directed proteomic analysis of the human nucleolus. Current biology: CB. 2002; 12:1–11. [PubMed: 11790298]

Barascu A, Le Chalony C, Pennarun G, Genet D, Imam N, Lopez B, Bertrand P. Oxidative stress induces an ATM-independent senescence pathway through p38 MAPK-mediated lamin B1 accumulation. The EMBO journal. 2012; 31:1080–1094. [PubMed: 22246186]

Bloom DA, Jaiswal AK. Phosphorylation of Nrf2 at Ser40 by protein kinase C in response to antioxidants leads to the release of Nrf2 from INrf2, but is not required for Nrf2 stabilization/accumulation in the nucleus and transcriptional activation of antioxidant response element-mediated NAD(P)H:quinone oxidoreductase-1 gene expression. The Journal of biological chemistry. 2003; 278:44675–44682. [PubMed: 12947090]

Boisvert FM, Ahmad Y, Gierlinski M, Charriere F, Lamont D, Scott M, Barton G, Lamond AI. A quantitative spatial proteomics analysis of proteome turnover in human cells. Molecular & cellular proteomics: MCP. 2012; 11 M111 011429.

Chan K, Lu R, Chang JC, Kan YW. NRF2, a member of the NFE2 family of transcription factors, is not essential for murine erythropoiesis, growth, and development. Proc Natl Acad Sci U S A. 1996; 93:13943–13948. [PubMed: 8943040]

Chua YS, Boh BK, Ponyeam W, Hagen T. Regulation of cullin RING E3 ubiquitin ligases by CAND1 in vivo. PloS one. 2011; 6:e16071. [PubMed: 21249194]

Constantinescu D, Gray HL, Sammak PJ, Schatten GP, Csoka AB. Lamin A/C expression is a marker of mouse and human embryonic stem cell differentiation. Stem cells (Dayton, Ohio). 2006; 24:177–185.

Dialynas G, Shrestha OK, Ponce JM, Zwerger M, Thiemann DA, Young GH, Moore SA, Yu L, Lammerding J, Wallrath LL. Myopathic lamin mutations cause reductive stress and activate the nrf2/keap-1 pathway. PLoS genetics. 2015; 11:e1005231. [PubMed: 25996830]

Duan S, Yuan G, Liu X, Ren R, Li J, Zhang W, Wu J. PTEN deficiency reprogrammes human neural stem cells towards a glioblastoma stem cell-like phenotype. Nature communications. 2015; 6:10068.

Endisha H, Merrill-Schools J, Zhao M, Bristol M, Wang X, Kubben N, Elmore LW. Restoring SIRT6 Expression in Hutchinson-Gilford Progeria Syndrome Cells Impedes Premature Senescence and Formation of Dysmorphic Nuclei. Pathobiology: journal of immunopathology, molecular and cellular biology. 2015; 82:9–20.

Fernandez P, Scaffidi P, Markert E, Lee JH, Rane S, Misteli T. Transformation resistance in a premature aging disorder identifies a tumor-protective function of BRD4. Cell reports. 2014; 9:248–260. [PubMed: 25284786]

Frost B, Hemberg M, Lewis J, Feany MB. Tau promotes neurodegeneration through global chromatin relaxation. Nature neuroscience. 2014; 17:357–366. [PubMed: 24464041]

Gabriel D, Roedl D, Gordon LB, Djabali K. Sulforaphane enhances progerin clearance in Hutchinson-Gilford progeria fibroblasts. Aging cell. 2015; 14:78–91. [PubMed: 25510262]

Gordon LB, Harten IA, Patti ME, Lichtenstein AH. Reduced adiponectin and HDL cholesterol without elevated C-reactive protein: clues to the biology of premature atherosclerosis in Hutchinson-Gilford Progeria Syndrome. The Journal of pediatrics. 2005; 146:336–341. [PubMed: 15756215]

Gordon LB, Rothman FG, Lopez-Otin C, Misteli T. Progeria: a paradigm for translational medicine. Cell. 2014; 156:400–407. [PubMed: 24485450]

Halaschek-Wiener J, Brooks-Wilson A. Progeria of stem cells: stem cell exhaustion in Hutchinson-Gilford progeria syndrome. The journals of gerontology Series A, Biological sciences and medical sciences. 2007; 62:3–8.

Hirota A, Kawachi Y, Yamamoto M, Koga T, Hamada K, Otsuka F. Acceleration of UVB-induced photoageing in nrf2 gene-deficient mice. Experimental dermatology. 2011; 20:664–668. [PubMed: 21569103]

Ibanez L, Ferrandiz ML, Brines R, Guede D. Effects of Nrf2 deficiency on bone microarchitecture in an experimental model of osteoporosis. 2014; 2014:726590.

Kubben N, Adriaens M, Meuleman W, Voncken JW, van Steensel B, Misteli T. Mapping of lamin A- and progerin-interacting genome regions. Chromosoma. 2012; 121:447–464. [PubMed: 22610065]

Kubben N, Brimacombe KR, Donegan M, Li Z, Misteli T. A high-content imaging-based screening pipeline for the systematic identification of anti-progeroid compounds. Methods (San Diego, Calif). 2015

Kubben N, Voncken JW, Demmers J, Calis C, van Almen G, Pinto Y, Misteli T. Identification of differential protein interactors of lamin A and progerin. Nucleus. 2010; 1:513–525. [PubMed: 21327095]

Kwon J, Han E, Bui CB, Shin W, Lee J, Lee S, Choi YB, Lee AH, Lee KH, Park C, et al. Assurance of mitochondrial integrity and mammalian longevity by the p62-Keap1-Nrf2-Nqo1 cascade. EMBO reports. 2012; 13:150–156. [PubMed: 22222206]

Lewis KN, Mele J, Hayes JD, Buffenstein R. Nrf2, a guardian of healthspan and gatekeeper of species longevity. Integrative and comparative biology. 2010; 50:829–843. [PubMed: 21031035]

Li J, Ichikawa T, Janicki JS, Cui T. Targeting the Nrf2 pathway against cardiovascular disease. Expert opinion on therapeutic targets. 2009; 13:785–794. [PubMed: 19530984]

Li W, Khor TO, Xu C, Shen G, Jeong WS, Yu S, Kong AN. Activation of Nrf2-antioxidant signaling attenuates NF-κB-inflammatory response and elicits apoptosis. Biochemical pharmacology. 2008; 76:1485–1489. [PubMed: 18694732]

Liu B, Ghosh S, Yang X, Zheng H, Liu X, Wang Z, Jin G, Zheng B, Kennedy BK, Suh Y, et al. Resveratrol rescues SIRT1-dependent adult stem cell decline and alleviates progeroid features in laminopathy-based progeria. Cell metabolism. 2012; 16:738–750. [PubMed: 23217256]

Liu GH, Barkho BZ, Ruiz S, Diep D, Qu J, Yang SL, Panopoulos AD, Suzuki K, Kurian L, Walsh C, et al. Recapitulation of premature ageing with iPSCs from Hutchinson-Gilford progeria syndrome. Nature. 2011a; 472:221–225. [PubMed: 21346760]

Liu GH, Suzuki K, Qu J, Sancho-Martinez I, Yi F, Li M, Kumar S, Nivet E, Kim J, Soligalla RD, et al. Targeted gene correction of laminopathy-associated LMNA mutations in patient-specific iPSCs. Cell stem cell. 2011b; 8:688–694. [PubMed: 21596650]

Liu Y, Rusinol A, Sinensky M, Wang Y, Zou Y. DNA damage responses in progeroid syndromes arise from defective maturation of prelamin A. Journal of cell science. 2006; 119:4644–4649. [PubMed: 17062639]

Lo SC, Hannink M. CAND1-mediated substrate adaptor recycling is required for efficient repression of Nrf2 by Keap1. Mol Cell Biol. 2006; 26:1235–1244. [PubMed: 16449638]

Low P. The role of ubiquitin-proteasome system in ageing. General and comparative endocrinology. 2011; 172:39–43. [PubMed: 21324320]

Ma Q. Role of nrf2 in oxidative stress and toxicity. Annual review of pharmacology and toxicology. 2013; 53:401–426.

Magesh S, Chen Y, Hu L. Small Molecule Modulators of Keap1-Nrf2-ARE Pathway as Potential Preventive and Therapeutic Agents. Medicinal Research Reviews. 2012; 32:687–726. [PubMed: 22549716]

Malhas AN, Lee CF, Vaux DJ. Lamin B1 controls oxidative stress responses via Oct-1. The Journal of cell biology. 2009; 184:45–55. [PubMed: 19139261]

Malhotra D, Portales-Casamar E, Singh A, Srivastava S, Arenillas D, Happel C, Shyr C, Wakabayashi N, Kensler TW, Wasserman WW, et al. Global mapping of binding sites for Nrf2 identifies novel targets in cell survival response through ChIP-Seq profiling and network analysis. Nucleic Acids Res. 2010; 38:5718–5734. [PubMed: 20460467]

Mateos J, De la Fuente A, Lesende-Rodriguez I, Fernandez-Pernas P, Arufe MC, Blanco FJ. Lamin A deregulation in human mesenchymal stem cells promotes an impairment in their chondrogenic potential and imbalance in their response to oxidative stress. Stem cell research. 2013; 11:1137–1148. [PubMed: 23994728]

McMahon M, Thomas N, Itoh K, Yamamoto M, Hayes JD. Redox-regulated turnover of Nrf2 is determined by at least two separate protein domains, the redox-sensitive Neh2 degron and the redox-insensitive Neh6 degron. The Journal of biological chemistry. 2004; 279:31556–31567. [PubMed: 15143058]

Michaeloudes C, Chang PJ, Petrou M, Chung KF. Transforming growth factor-beta and nuclear factor E2-related factor 2 regulate antioxidant responses in airway smooth muscle cells: role in asthma.

American journal of respiratory and critical care medicine. 2011; 184:894–903. [PubMed: 21799075]

Miller CJ, Gounder SS, Kannan S, Goutam K, Muthusamy VR, Firpo MA, Symons JD, Paine R 3rd, Hoidal JR, Rajasekaran NS. Disruption of Nrf2/ARE signaling impairs antioxidant mechanisms and promotes cell degradation pathways in aged skeletal muscle. Biochimica et biophysica acta. 2012; 1822:1038–1050. [PubMed: 22366763]

Murakami S, Shimizu R, Romeo PH, Yamamoto M, Motohashi H. Keap1-Nrf2 system regulates cell fate determination of hematopoietic stem cells. Genes to cells: devoted to molecular & cellular mechanisms. 2014; 19:239–253. [PubMed: 24580727]

Musich PR, Zou Y. Genomic instability and DNA damage responses in progeria arising from defective maturation of prelamin A. Aging. 2009; 1:28–37. [PubMed: 19851476]

Osorio FG, Barcena C, Soria-Valles C, Ramsay AJ, de Carlos F, Cobo J, Fueyo A, Freije JM, Lopez-Otin C. Nuclear lamina defects cause ATM-dependent NF-kappaB activation and link accelerated aging to a systemic inflammatory response. Genes & development. 2012; 26:2311–2324. [PubMed: 23019125]

Pacheco LM, Gomez LA, Dias J, Ziebarth NM, Howard GA, Schiller PC. Progerin expression disrupts critical adult stem cell functions involved in tissue repair. Aging. 2014; 6:1049–1063. [PubMed: 25567453]

Pan H, Guan D, Liu X, Li J, Wang L, Wu J, Zhou J, Zhang W, Ren R, Zhang W, et al. SIRT6 safeguards human mesenchymal stem cells from oxidative stress by coactivating NRF2. Cell research. 2016

Pegoraro G, Kubben N, Wickert U, Gohler H, Hoffmann K, Misteli T. Ageing-related chromatin defects through loss of the NURD complex. Nat Cell Biol. 2009; 11:1261–1267. [PubMed: 19734887]

Pegoraro G, Voss TC, Martin SE, Tuzmen P, Guha R, Misteli T. Identification of mammalian protein quality control factors by high-throughput cellular imaging. PloS one. 2012; 7:e31684. [PubMed: 22363705]

Pekovic V, Gibbs-Seymour I, Markiewicz E, Alzoghaibi F, Benham AM, Edwards R, Wenhert M, von Zglinicki T, Hutchison CJ. Conserved cysteine residues in the mammalian lamin A tail are essential for cellular responses to ROS generation. Aging cell. 2011; 10:1067–1079. [PubMed: 21951640]

Pickering AM, Staab TA, Tower J, Sieburth D, Davies KJ. A conserved role for the 20S proteasome and Nrf2 transcription factor in oxidative stress adaptation in mammals, Caenorhabditis elegans and Drosophila melanogaster. The Journal of experimental biology. 2013; 216:543–553. [PubMed: 23038734]

Rankin J, Ellard S. The laminopathies: a clinical review. Clin Genet. 2006; 70:261–274. [PubMed: 16965317]

Richards SA, Muter J, Ritchie P, Lattanzi G, Hutchison CJ. The accumulation of un-repairable DNA damage in laminopathy progeria fibroblasts is caused by ROS generation and is prevented by treatment with N-acetyl cysteine. Hum Mol Genet. 2011; 20:3997–4004. [PubMed: 21807766]

Rivera-Torres J, Acin-Perez R, Cabezas-Sanchez P, Osorio FG, Gonzalez-Gomez C, Megias D, Camara C, Lopez-Otin C, Enriquez JA, Luque-Garcia JL, et al. Identification of mitochondrial dysfunction in Hutchinson-Gilford progeria syndrome through use of stable isotope labeling with amino acids in cell culture. Journal of proteomics. 2013; 91:466–477. [PubMed: 23969228]

Rodriguez S, Coppede F, Sagelius H, Eriksson M. Increased expression of the Hutchinson-Gilford progeria syndrome truncated lamin A transcript during cell aging. European journal of human genetics: EJHG. 2009; 17:928–937. [PubMed: 19172989]

Rosengardten Y, McKenna T, Grochova D, Eriksson M. Stem cell depletion in Hutchinson-Gilford progeria syndrome. Aging cell. 2011; 10:1011–1020. [PubMed: 21902803]

Scaffidi P, Misteli T. Lamin A-dependent nuclear defects in human aging. Science. 2006; 312:1059–1063. [PubMed: 16645051]

Scaffidi P, Misteli T. Lamin A-dependent misregulation of adult stem cells associated with accelerated ageing. Nat Cell Biol. 2008; 10:452–459. [PubMed: 18311132]

Steel R, Cowan J, Payerne E, O'Connell MA, Searcey M. Anti-inflammatory Effect of a Cell-Penetrating Peptide Targeting the Nrf2/Keap1 Interaction. ACS Medicinal Chemistry Letters. 2012; 3:407–410. [PubMed: 22582137]

Tanaka Y, Aleksunes LM, Yeager RL, Gyamfi MA, Esterly N, Guo GL, Klaassen CD. NF-E2-related factor 2 inhibits lipid accumulation and oxidative stress in mice fed a high-fat diet. The Journal of pharmacology and experimental therapeutics. 2008; 325:655–664. [PubMed: 18281592]

Ungvari Z, Bagi Z, Feher A, Recchia FA, Sonntag WE, Pearson K, de Cabo R, Csiszar A. Resveratrol confers endothelial protection via activation of the antioxidant transcription factor Nrf2. American Journal of Physiology - Heart and Circulatory Physiology. 2010; 299:H18–24. [PubMed: 20418481]

Viteri G, Chung YW, Stadtman ER. Effect of progerin on the accumulation of oxidized proteins in fibroblasts from Hutchinson Gilford progeria patients. Mech Ageing Dev. 2010; 131:2–8. [PubMed: 19958786]

Voncken JW, Niessen H, Neufeld B, Rennefahrt U, Dahlmans V, Kubben N, Holzer B, Ludwig S, Rapp UR. MAPKAP kinase 3pK phosphorylates and regulates chromatin association of the polycomb group protein Bmi1. The Journal of biological chemistry. 2005; 280:5178–5187. [PubMed: 15563468]

Wang XJ, Hayes JD, Wolf CR. Generation of a stable antioxidant response element-driven reporter gene cell line and its use to show redox-dependent activation of nrf2 by cancer chemotherapeutic agents. Cancer Res. 2006; 66:10983–10994. [PubMed: 17108137]

Yoh K, Itoh K, Enomoto A, Hirayama A, Yamaguchi N, Kobayashi M, Morito N, Koyama A, Yamamoto M, Takahashi S. Nrf2-deficient female mice develop lupus-like autoimmune nephritis. Kidney international. 2001; 60:1343–1353. [PubMed: 11576348]

Zakkar M, Van der Heiden K, Luong le A, Chaudhury H, Cuhlmann S, Hamdulay SS, Krams R, Edirisinghe I, Rahman I, Carlsen H, et al. Activation of Nrf2 in endothelial cells protects arteries from exhibiting a proinflammatory state. Arteriosclerosis, thrombosis, and vascular biology. 2009; 29:1851–1857.

Zhang J, Lian Q, Zhu G, Zhou F, Sui L, Tan C, Mutalif RA, Navasankari R, Zhang Y, Tse HF, et al. A human iPSC model of Hutchinson Gilford Progeria reveals vascular smooth muscle and mesenchymal stem cell defects. Cell stem cell. 2011; 8:31–45. [PubMed: 21185252]

Zhang W, Li J, Suzuki K, Qu J, Wang P, Zhou J, Liu X, Ren R, Xu X, Ocampo A, et al. Aging stem cells. A Werner syndrome stem cell model unveils heterochromatin alterations as a driver of human aging. Science. 2015; 348:1160–1163. [PubMed: 25931448]

Zhao Z, Chen Y, Wang J, Sternberg P, Freeman ML, Grossniklaus HE, Cai J. Age-related retinopathy in NRF2-deficient mice. PloS one. 2011; 6:e19456. [PubMed: 21559389]

Highlights

- Impaired activity of the NRF2 antioxidative pathway is a driver mechanism in HGPS
- Suppressed NRF2 activity and oxidative stress recapitulate HGPS aging defects
- Re-activation of NRF2 decreases oxidative stress and reverses cellular HGPS defects

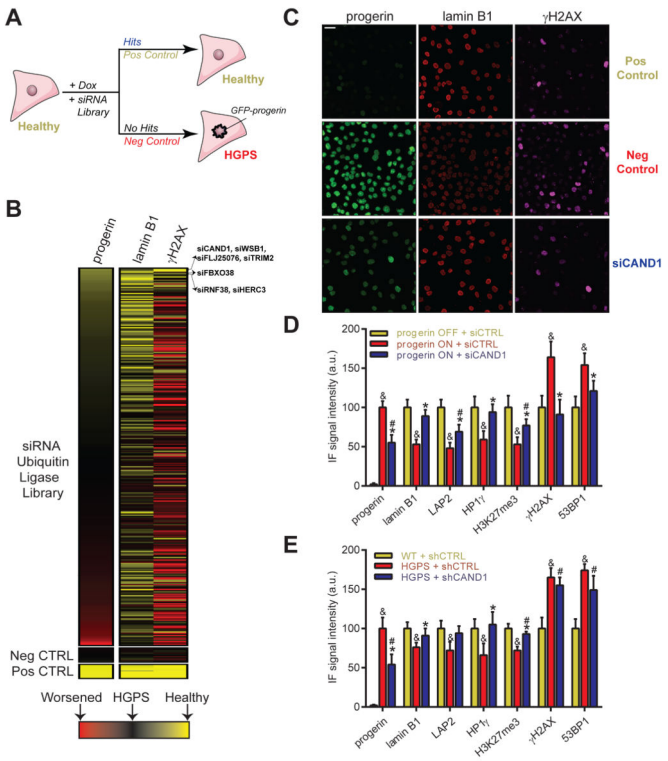

Fig 1. High-throughput RNAi screen identifies CAND1 as a mediator of progerin-induced aging

(A) Schematic and **(B)** heatmap representation of RNAi screen, indicating identified candidates (Fig S1J, Table S2). **(C)** Representative IF images for CAND1 RNAi and controls in progerin inducible fibroblasts (See Experimental procedures). Scale bar: 25μm. **(D)** IF quantification in inducible or **(E)** WT and HGPS fibroblasts. $p<0.05$: $^{\&}$ ONorHGPS/siCTRL vs. OFForWT/siCTRL; $^{\#}$ ONorHGPS/siCAND1 vs. OFForWT/siCTRL; * ONorHGPS/siCAND1 vs. ONorHGPS/siCTRL. N>300; values represent averages ± SD from at least 3 experiments.

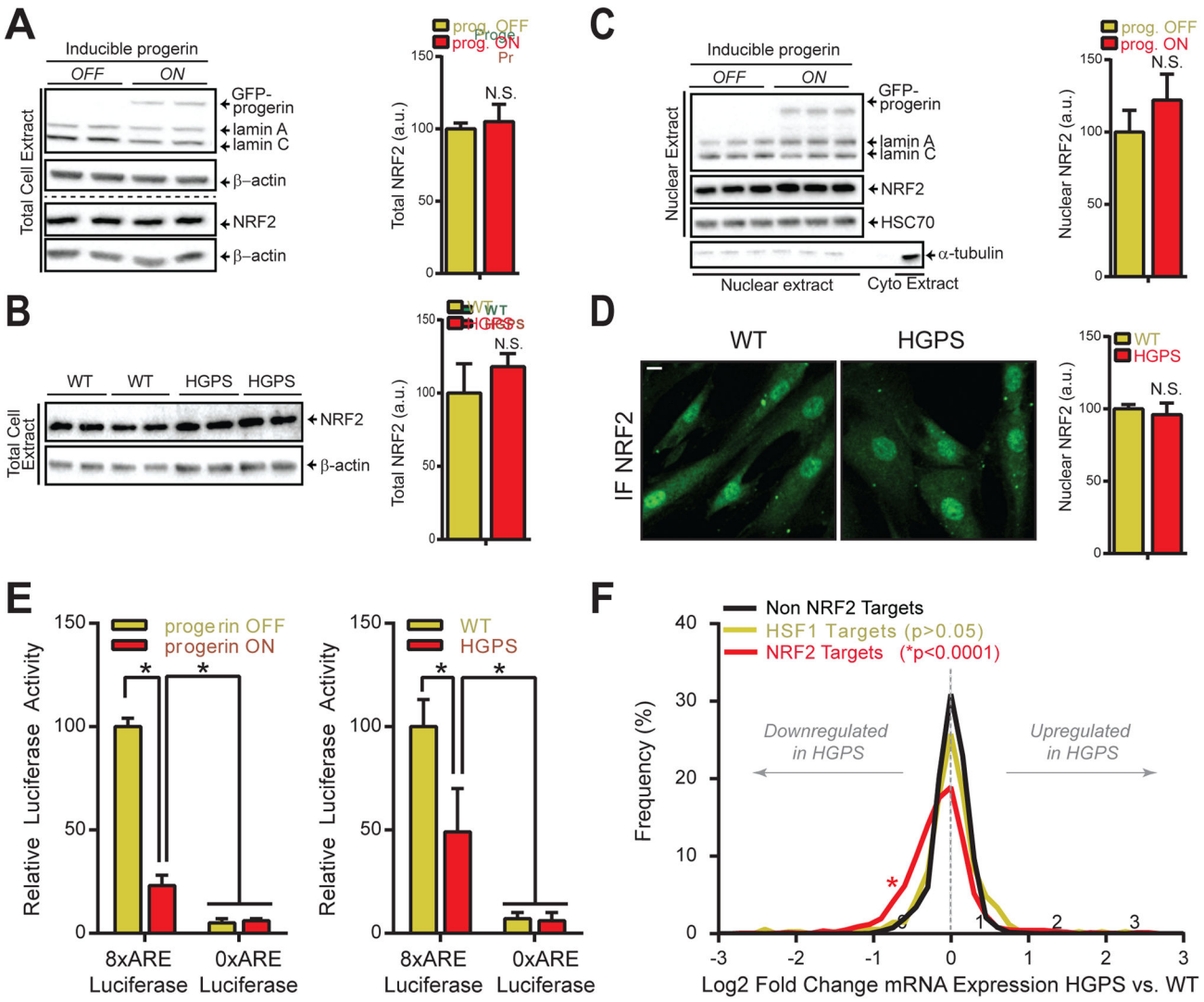

Fig 2. NRF2 transcriptional activity is impaired in HGPS

(A) Western blot (WB) analysis of total progerin inducible fibroblasts (P1 cells, See Experimental Procedures) extracts (2 biological replicates). Dotted line indicates separate WBs. **(B)** WB of total cell extract of WT and HGPS fibroblast (2 biological replicates for 4 cell lines, see Experimental Procedures). **(C)** WB of nuclear P1 cell extract (3 biological replicates of P1 cells). α-tubulin serves as cytoplasmic control. **(D)** NRF2 IF staining (Abcam 62352) in formaldehyde fixed WT and HGPS fibroblasts. N>300; Scale bar: 10μm. **(E)** ARE-luc assay (See Experimental procedures). *p<0.05. **(F)** Line graph of Log2 mRNA expression changes between WT and HGPS fibroblasts for indicated transcriptional targets. A left-shift of the NRF2-targets plot indicates an increased frequency of NRF2 regulated target genes that are downregulated in HGPS patients (p<0.0001).

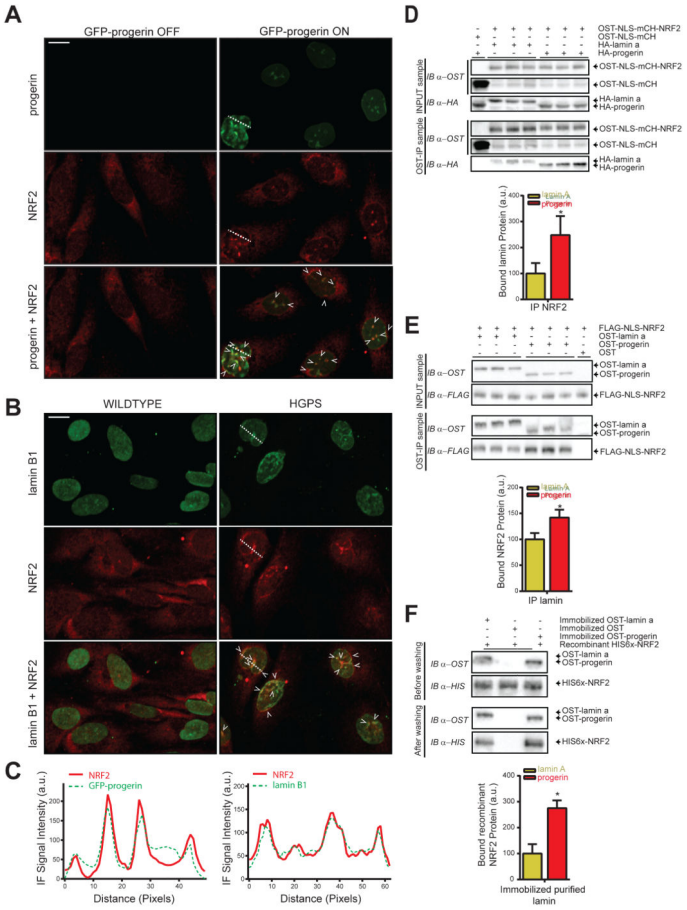

Fig 3. Progerin mislocalizes NRF2

(A) NRF2 IF staining (Sc-722) in methanol fixed progerin indicuble fiborblasts (P1 cells, See Experimental Procedures). Arrows indicate overlapping IF signals. Scale bar: 10μm. **(B)** IF stain for NRF2 (Sc-722) and lamin B1 (Sc-6217) in methanol fixed WT and HGPS fibroblasts. Arrows indicate overlapping IF signals. Scale bar: 10μm. **(C)** Line graphs indicating IF signal intensity across the dotted lines in panel A and B. **(D)** WB analysis of interaction between immunoprecipitated OST-NLS-mCherry-NRF2 with HA-lamin A or HA-progerin, or **(E)** immunoprecipitated OST-lamin A and OST-progerin with FLAG-NLS-NRF2 in HEK293FT cells (3 biological replicates; See Experimental Procedures). *p<0.05. **(F)** WB analysis to probe the interaction between WT immunoprecipitated OST-lamin A or OST-progerin with recombinant HIS6x- NRF2. * p<0.05.

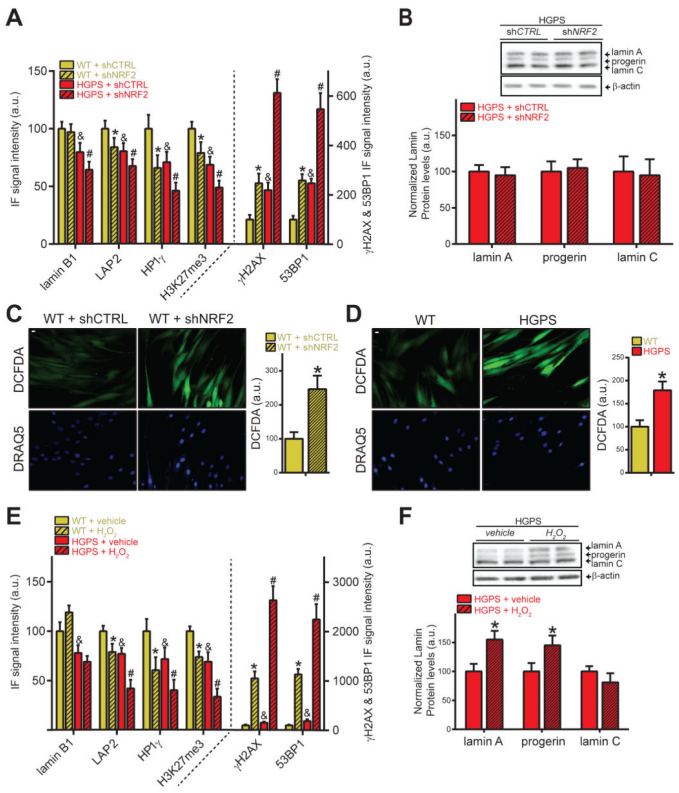

Fig 4. NRF2 impairment causes oxidative stress and recapitulates the progeroid phenotype

(A) IF analysis in WT and HGPS fibroblasts. p<0.05: & WT/shCTRL vs. HGPS/shCTRL; * WT/shCTRL vs. WT/shNRF2; #, HGPS/shCTRL vs. HGPS/shNRF2. **(B)** WB analysis of HGPS fibroblasts (2 biological replicates). **(C)** DCFDA-based ROS quantification in WT fibroblasts expressing indicated shRNAs or **(D)** in WT and HGPS fibroblasts (N>300; *p<0.05). Scale bar: 10 μm. **(E)** IF analysis in WT and HGPS fibroblasts treated with H_2O_2 (250μM; 4 days). p<0.05: &WT/vehicle vs. HGPS/vehicle; *WT/vehicle vs. WT/H_2O_2; #HGPS/vehicle vs. HGPS/H_2O_2. **(F)** WB analysis of HGPS fibroblasts treated with H_2O_2 (250μM; 4 days) (2 biological replicates).*, p<0.05. For all IF-based panels: N>300; values represent averages ± SD from at least 3 experiments.

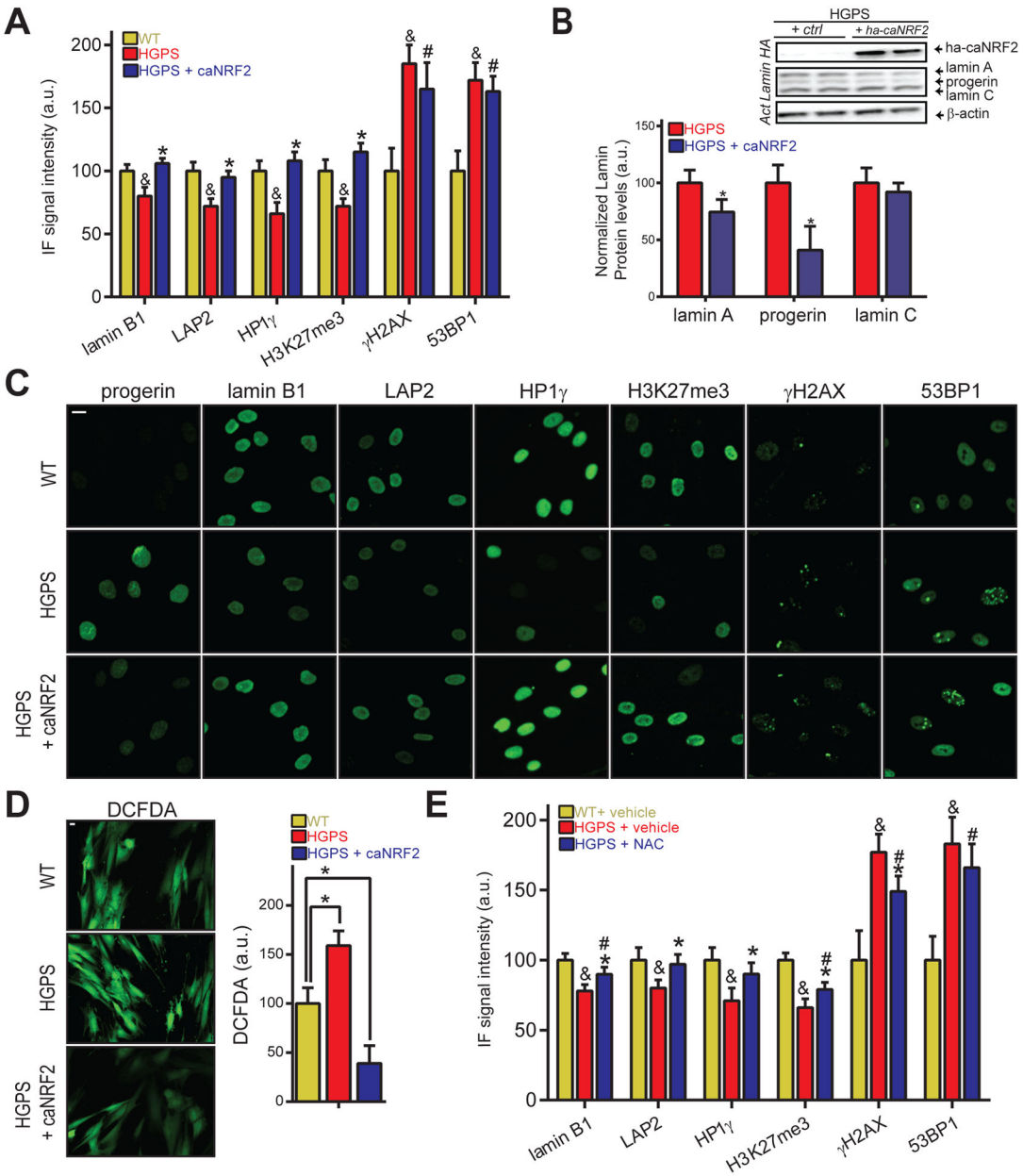

Fig 5. Reactivation of NRF2 restores aging defects in HGPS patient fibroblasts

(A) IF analysis in WT or HGPS fibroblasts expressing control or caNRF2 for 96 hours. $p<0.05$: $^{\&}$ WT/CTRL vs. HGPS/CTRL; *HGPS/CTRL vs. HGPS/caNRF2; $^{\#}$WT/CTRL vs. HGPS/caNRF2. **(B)** WB analysis of HGPS fibroblasts (2 biological replicates). *$p<0.05$ HGPS vs HGPS/caNRF2 **(C)** Representative IF stain for panel A. Scale bar: 10μm. **(D)** DCFDA-based ROS quantification in CTRL or caNRF2 expressing WT and HGPS fibroblasts. **(E)** IF analysis of 96 hour vehicle or NAC-treated WT and HGPS fibroblasts. $p<0.05$: $^{\&}$WT/vehicle vs. HGPS/vehicle. *HGPS/vehicle vs. HGPS/NAC. $^{\#}$WT/vehicle vs. HGPS/NAC. For all IF-based panels: N>300; values represent averages ± SD from at least 3 experiments.

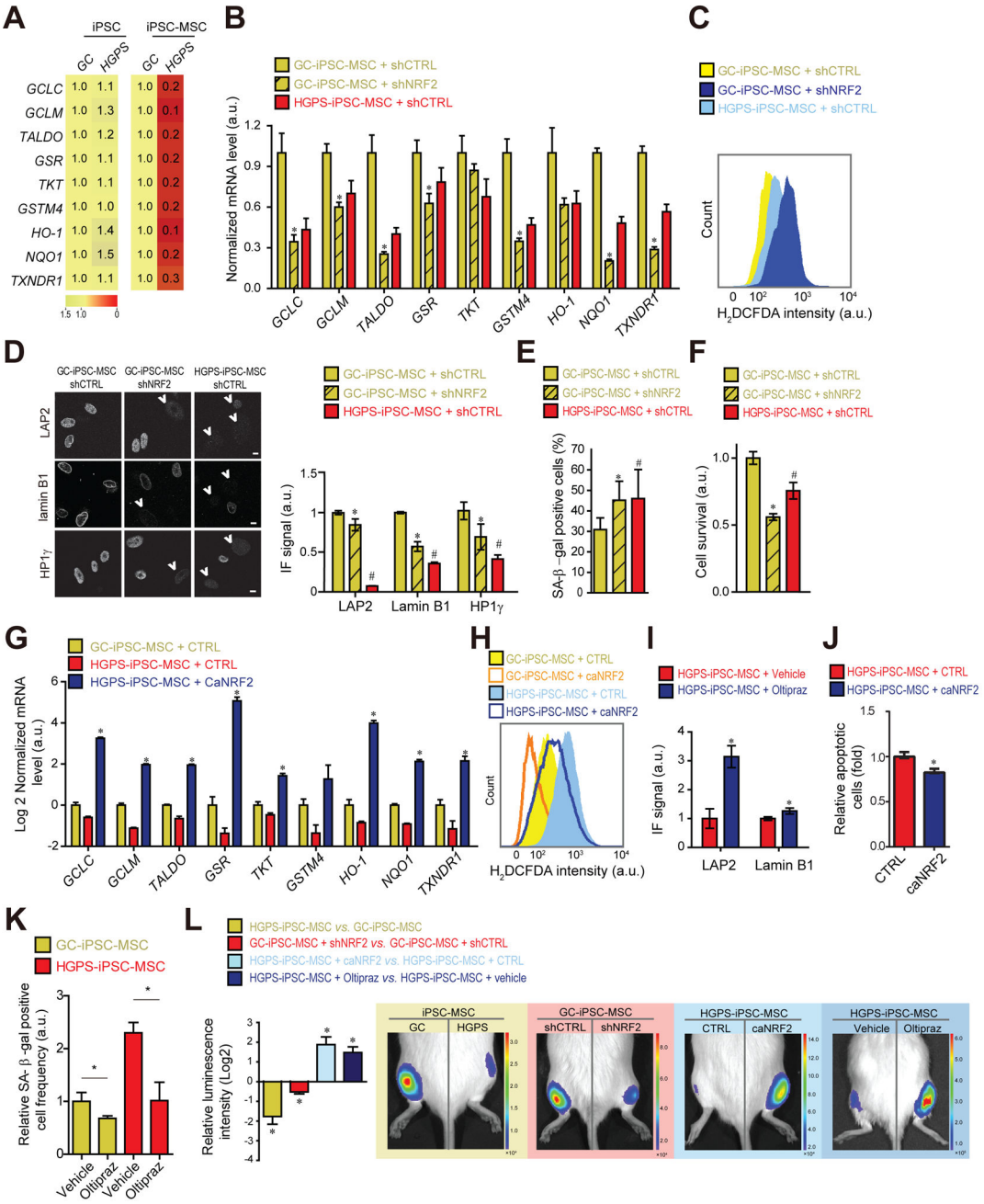

Fig 6. NRF2 activation alleviates HGPS mesenchymal stem cell viability defects

(A) Heatmap of NRF2-target mRNA expression levels. Values represent averages from at least 3 experiments. **(B)** NRF2 target mRNA expression. *p<0.05, GC/shCTRL vs. GC/shNRF2. **(C)** H2DCFDA-based ROS quantification. **(D)** IF analysis of lamin B1 (manual count of low lamin expressing B1 cells), LAP2 and HP1γ (See experimental Procedures). Scale bar: 10 μm. N>300. P<0.05: *GC/shCRTL vs. GC/shNRF2; #GC/shCRTL vs. HGPS/shCTRL. **(E)** Frequency of SA-β-gal positive cells and **(F)** relative cell survival rate (See Experimental Procedures). p<0.05: *GC/shCRTL vs. GC/shNRF2; #GC/shCTRL vs. HGPS/shCTRL. **(G)** NRF2-target mRNA expression levels. *p<0.05, HGPS/CTRL vs. HGPS/

caNRF2. **(H)** H2DCFDA-based ROS quantification for indicated cell types. **(I)** IF quantification (See panel D) in vehicle or Oltipraz treated (20 μM; 3 weeks) HGPS-iPSC-MSCs. N>100. *p<0.05. **(J)** Relative amounts of apoptotic cells and **(K)** SA-β-galactosidase positive cells in GC- and HGPS-iPSC-MSC expressing caNRF2 or treated with Oltipraz (20 μM; 3 weeks). N>300. *p<0.05. **(L)** *In vivo* MSC implantation assay for indicated conditions (Oltipraz: 20 μM; 3 wks) (N=3–5). *p<0.05 for indicated comparisons: HGPS vs. GC; GC/shNRF2 vs. GC/shCTRL; HGPS/caNRF2 vs. HGPS/CTRL; HGPS/Oltipraz vs. HGPS/Vehicle. For all bar-graphs values represent averages ± SD from at least 3 experiments.